Fuel 311 (2022) 122148

Contents lists available at ScienceDirect

Fuel

journal homepage: www.elsevier.com/locate/fuel

Micro-fractures in coal induced by high pressure CO_2 gas fracturing

Yunxing Cao [a,b,c,d,*], Junsheng Zhang [a,b,c,d], Xinsheng Zhang [a], Shimin Liu [e], Derek Elsworth [e]

[a] Institute of Resources & Environment, Henan Polytechnic University, Jiaozuo 454000, China
[b] Collaborative Innovation Center of Coalbed Methane and Shale Gas for Central Plains Economic Region, Henan Province, Henan Polytechnic University, Jiaozuo 454000, China
[c] Henan International Joint Laboratory for Unconventional Energy Geology and Development, Henan Polytechnic University, Jiaozuo 454000, China
[d] Gas Geology and Engineering Research Center, Henan Polytechnic University, Jiaozuo 454000, China
[e] Department of Energy and Mineral Engineering, G^3 Center and Energy Institute, Pennsylvania State University, University Park, PA 16802, United States

ARTICLE INFO

Keywords:
Gas drainage
CO_2 gas fracturing
Coal damage
Complex fracture network

ABSTRACT

To effectively drain gas from coal seam, many technologies have been developed to fracture the coal which in turn to release the formation stress and increase permeability and finally achieve the desired gas drainage. CO_2 gas fracturing is a newly developed technique for coal seam stimulation towards effective gas drainage. This technique can provide radial fracturing from centimeter to meters scales, but the small-scale fracture system that feeds into this radial system, at millimeter to micrometer scale, has not previously been systematically studied for quantifying the matrix damages. This study addresses this deficiency through blast-loading experiments with CO_2 on anthracite specimens at overpressures of 120 MPa, 150 MPa and 185 MPa in the in-house novel experimental system. The Field Emission Scanning Electron Microscope (FESEM) images suggest that the cleat system is destroyed, and the intervening matrix effectively pulverized due to the impact load induced by the CO_2 blasting. Radial and branching fractures are featured with the process, as typical in high velocity fracturing. The center point is a serious damage mark (DM) that always shows as a shallow pit, and number of smaller broken coal scatter surround the mark. These newly produced fractures are open and zigzag. Based on the observations, it is supposed that the matrix fracturing mechanism by CO_2 gas impacting can be described as four consecutive steps: CO_2 gas beam destroyed cleat system firstly, and coal broken to millimeter size particles. Meanwhile, CO_2 gas jet beam impacting on coal matrix induce a DM and resulting in the matrix's tensile deformation. Consequently, tri-fracture initiated from the DM and extending radially to different direction. When numerical tri-fracture connected and formed a complex fracture network in which permeability is expected to be significantly promoted for the effective gas drainage.

1. Introduction

Coal mine gas accidents, such gas explosions and gas-coal outbursts, are the major mining safety challenge for the Chinese coal industry. From 1949 to 2009, 25 severe coal mine accidents were reported with more than 100 fatalities per event. Out of these 25 mine disasters, 19 accidents were recognized as gas explosions or gas-coal outbursts [1–3]. By 2012, it was estimated that 3700 coal mines of 12,880 mines (~28%) were classified as gassy or outburst prone mines [4]. Gas related coal mine hazards are expected to worsen as mining depths progressively increase towards 1500 m [5,6].

Effective gas drainage is therefore a pre-requisite for safe mining to reduce gas content to a minimal level that ventilation system can accommodate [7–11]. Various technologies for gas drainage have been developed and implemented over the last century to mitigate gas related geohazards [12]. Common gas drainage technologies include: in-seam closely-spaced borehole drainage, hydraulic fracturing [13,14], in-seam hydraulic cavity formation and flushing [15–20], deep borehole explosive blasting [21], under-seam roadway drainage [22] and over-seam gallery drainage [23] together with the provision of dense arrays of in-seam boreholes [24,25]. These engineering interventions all attempt to effectively drain the gas in a cost-effective and timely manner and to thereby reduce formation gas content to an acceptable level.

CO_2 fracturing is a waterless stimulation technique [26–29] that has shown significant promise – mainly due to unique CO_2-coal interactions. CO_2 is being the idea gas medium for the nonflammable blasting because

* Corresponding author at: 2001 Shiji Aveniew, Jiaozuo, Henan 454000, China.
E-mail address: yxcao17@126.com (Y. Cao).

https://doi.org/10.1016/j.fuel.2021.122148
Received 19 April 2021; Received in revised form 16 September 2021; Accepted 28 September 2021
Available online 27 December 2021

it is safe and has triple point at 31.04 °C. As the invading CO_2 displaces the methane by counter-diffusion, it leaves the gas pathway undamaged - as compared to water-based fracturing fluids. CO_2 fracturing has been successfully applied in Shanxi and Guizhou provinces and Inner Mongolia since 2012. It is our estimated that this technology has enabled more than 250 km of coal seam roadways to be safely excavated in Shanxi and Guizhou provinces. CARDOX-based CO_2 fracturing has been successfully applied in tens of outburst-prone coal mines in China since 2012 and with impressive outcomes [28]. Multiple forensic observations of CO_2-fractured seams have shown that the coal seam can be effectively fractured - with radial fractures from borehole commonly observed in situ. This, together with measurements of gas drainage, confirms that CO_2 fracturing can be an effective technique for gas drainage.

Despite this success, mechanisms and controls on fracturing during the dynamic process remain poorly constrained. Although CO_2 fracturing can effectively produce fractures at meter-to-nanometer scales, the portioning of damage between the gas-overpressure and the dynamic body wave remains unclear – inhibiting the optimization of design for greater reach and improved surface area in the fracture network – two features that would maximize gas recovery. The first description of the fracture system generated by CO_2 -gas-fracturing was reported by Cao, et al. [28], but focused only on fractures at centimeter-to-meter scale and only from limited underground observations. These centimeter-to-meter scale fracture networks provide improved gas pathways, as indexed by an apparent increase in formation permeability. However, through in-mine coal sampling, it is also evident that CO_2 fracturing produces an extensive network of millimeter-to-micron scale fractures – likely impacting texture to nanometer-scale. However, no systematic evaluation has been conducted of these micron-scale fracture networks.

In this study, micrometer scale (micro-scale) fractures produced through CO_2-blasting laboratory experiments are characterized and evaluated. Field emission scanning electron microscopy (FESEM) is employed as a probing tool to semi-quantitatively characterize damage at micron-to-nano scale and to provide mechanistic interpretations of network formation. This study provides an advanced understanding on the micromechanics of coal damage under blasting load. This study can shed light on the CO_2 fracturing multi-scale damage mechanism and offer a unique explanation on the effectiveness of CO_2 fracturing on coal drainage efficiency.

2. Geological setting of Yuxi coal mine

Samples are recovered from the Yuxi coal mine, located in the south-eastern limb of the Qinshui syncline, Shanxi province, China (Fig. 1). The mine accesses coal bearing strata of the Shanxi formation (P_{1s}) of lower Permian that comprises six coal seams reaching a combined thickness of ~ 50 m. The objective of this study is Coal 3# with thickness varying from 5.12 ~ 7.20 m with an average of 5.85 m.

The geological structure of the 3# seam is simple with only small normal faults and simple folds observed by 3D seismic. The first working longwall face, face 1301, was planned for the center of the mine. The working face is 1250 m long and 200 m wide (Fig. 1). To efficiently dilute methane content, three return roadways and two inlet roadways were designed to access the longwall working face.

3. Sample preparation and experimental apparatus

3.1. Coal sampling and preparation

Fresh coal samples were collected from the 3# coal seam in the Yuxi coal mine. Fresh block samples (Fig. 2A) were collected from the active mine working face and transported to the lab for the analyses. Proximate analysis and ultimate analysis of the coal samples were conducted according to China National Standards GB/T 31391–2015 and GB/T 212–2008, the results are listed in Tables 1 and 2. As shown, volatile and maximum vitrinite reflectance were determined as 8.07% and $R_{o,max}$ = 3.36% - indicating the coal as anthracite in type.

Cylindrical coal core specimens with the dimension of ϕ50 × 100 mm was prepared using a wire cutting machine (Fig. 2B and 2C1) by

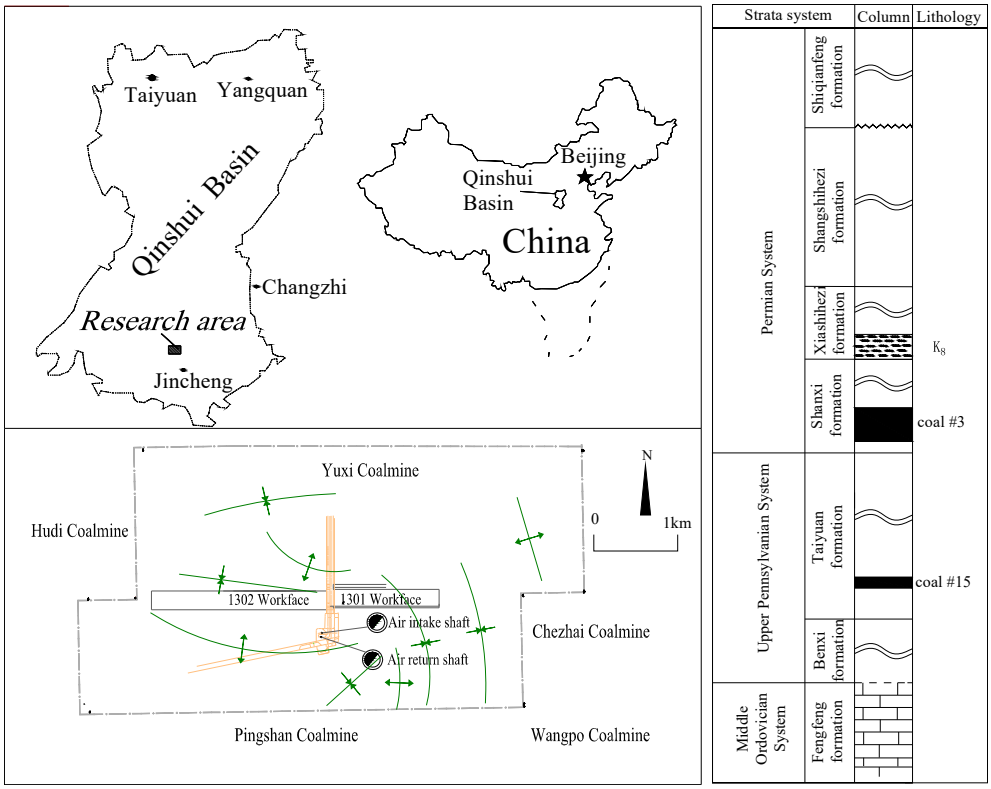

Fig. 1. Geology of the coal mine and location of coal sampling location.

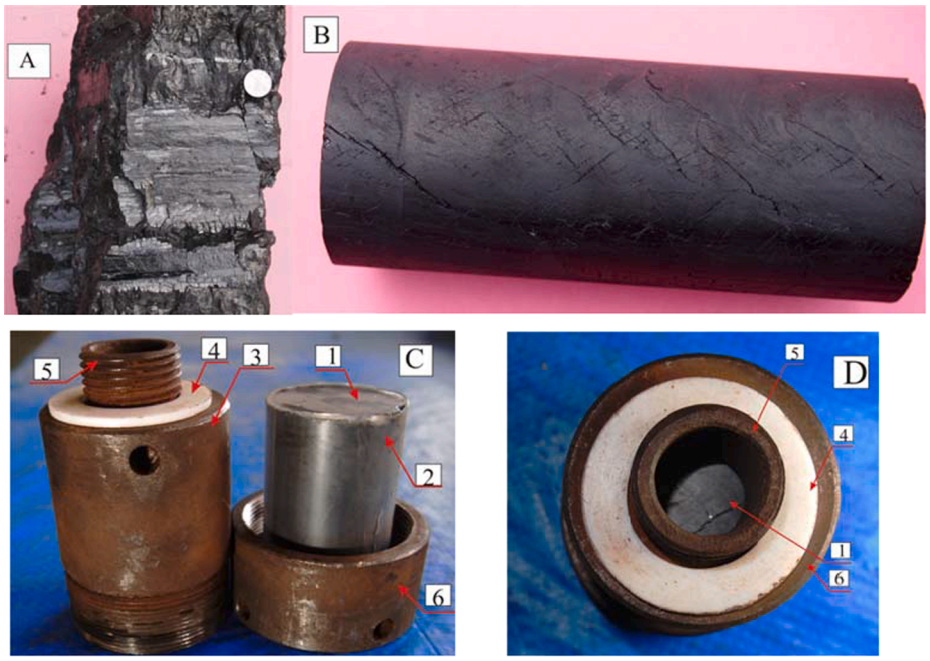

Fig. 2. Original coal blocks and prepared cylindrical specimen. Note: A, virgin coal block sample before cylindrical specimen preparation; B, cylindrical specimen (diameter of 50 mm and length of 100 mm) prepared using a wire cutting machine; C, test specimen jacket including C1- coal test specimen; C2– thermoplastic jacket to contain the sample; C3-steel core holder; C4- sealant within anulus; C5-CO_2 gas ejecting nozzle; C6-steel cap to seal the end of the core holder. D1 = C1, cylindrical specimen; D4 = C4, sealant within anulus; D5 = C5, CO_2 gas ejecting nozzle; D6 = C6, steel cap to seal the end of the core holder.

Table 1
Proximate analyses of the coal sample.

$R_{o,max}$(%)	M_{ad} (%)	A_{ad} (%)	V_{daf} (%)	VD_{ad} ($t•m^{-3}$)
2.9–3.73	0.86–4.34	11.74–17.76	7.43–9.17	1.31–1.53
3.36	2.37	14.28	8.07	1.49

$R_{o,max}$: vitrinite maximum reflectance ; M_{ad}: air dry moisture content; A_{ad}: air dry ash yield; V_{daf} : dry ash free volatile matter; VD_{ad}: air dry volume density.

Table 2
Ultimate analysis of the coal sample.

C_{ad}/(%)	H_{ad}/(%)	O_{ad}/(%)	N_{ad}/(%)	O_{daf}/(%)
82.90	2.90	2.46	1.15	2.46

cutting along the bedding direction. The cylindrical specimen was first fitted within a thermoplastic jacket (Fig. 2 C2) to prevent collapse, and then placed in a steel core holder (Fig. 2 C3). The head of the specimen (Fig. 2 C1) is open to the high-pressure CO_2 discharged from a nozzle (Fig. 2 C5) and impacting the sample with the base of the steel core holder sealed with a steel cap (Fig. 2 C6).

3.2. CO_2 gas blasting apparatus

The CO_2 gas blasting device designed and manufactured for this specific experiment is shown in Fig. 3. The device contains: (1) a large steel blasting chamber with a diameter of 1500 mm and a length of 3000 mm. The steel chamber was isolated within a sandbag box (1800 × 1800 × 3000 mm) to protect against accidental rupture. All blasting operations carried out in the chamber are isolated for safety (Fig. 3A). (2) a 2000 mm long steel test pipe (Fig. 3B) with OD 140 mm and ID 94 mm to a fix the CARDOX blasting system. This is sealed at its two ends with a steel case (Fig. 3B). (3) a CARDOX system for CO_2 blasting. This includes a CARDOX tube (Fig. 3B3 and C8) containing liquid CO_2 (Fig. 3C9), and a chemical heater (Fig. 3C10) to energize the CARDOX tool by vaporizing the liquid CO_2 behind a rupture disc (Fig. 3C7) that limits the blasting pressure, and a discharge head (Fig. 3C6) to discharge high pressure CO_2 to impact the coal sample (Fig. 3C1), and a firing head (Fig. 3C11) to ignite the heater. The CARDOX tube is charged with 2.2 kg of liquid CO_2. The designated pressures of the CO_2 are selected as 120 MPa, 150 MPa and 185 MPa as limited by the selection of the rupture discs. (4) Two diametrically opposed cylindrical steel core holders (Fig. 3C3) were fixed at the end of the steel test pipe with the ends open and facing to the CARDOX discharge nozzle (Fig. 3C4); (5) Two cylindrical coal samples (Fig. 3C1) are loaded into the specimen cases with the flat end of each coal sample facing the CARDOX discharge head nozzle to facilitate gas impact, The distance between nozzle and the coal is about 35 mm. In total, 12 coal samples were impacted with different pressures.

Photo A: Safety blasting chamber for CO_2 coal impact experiments: A1- sandbag isolation chamber; A2- inner room of the blasting chamber; A3 - blasting test pipe; A4- CARDOX tube held in the blasting test pipe.

Photo B: Blasting test pipe inside the safety chamber: B1- test pipe; B2- the two steel core holders, B3- the CARDOX tube, B4- the discharge port in the discharge head for high pressure CO_2 gas blasting and impact loading on the coal sample.

Sketch C: CO_2 blasting test system including test pipe, CARDOX system and core holders. C1- coal sample; C2– thermoplastic jacket containing the coal sample; C3– steel core holder for the thermoplastic case; C4- pressure gas through-hole in steel pipe connecting discharge port and coal sample; C5- high pressure CO_2 gas discharge port; C6- discharge head; C7- rupture disc; C8- CARDOX tube; C9- liquid CO_2 within the tube; C10- chemical heater; C11- firing head; C12- blasting test pipe; C13- fixed member for fixing the test pipe; C14- sealing caps at the two ends of the test pipe. C5-C11 comprise the CARDOX system containing the 2.2 kg of liquid CO_2 used in this study.

3.3. CO_2 gas blasting procedure

The following procedures were repeated in each experiment:

(1) Fix the steel pipe into the holder system within the blasting chamber.
(2) Set and fix the CARDOX tube in the steel pipe.
(3) Set the coal specimens within the thermoplastic jacket and load samples into the twin opposing core holders with sample-top faces open and facing the blasting nozzle.
(4) Ignite the heater in the CARDOX tube. The chemical heater provides thermal energy heating the liquid CO_2 transforming to

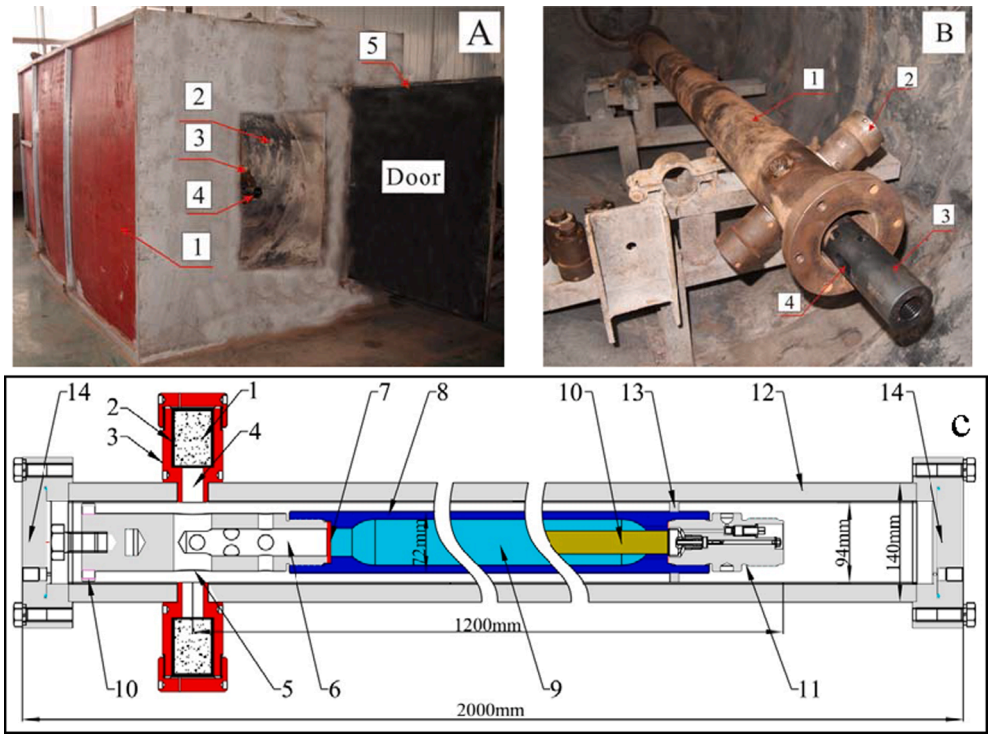

Fig. 3. Laboratory CO_2 blasting device and major components.

supercritical CO_2, which then discharge out of the tube in high pressure CO_2 gas phase to directly impact the coal specimen through discharge port in the discharge head. Fracture the coal.

(5) Collect specimens from the impacted sample for FESEM analysis.

3.4. Scanning electron microscope

A field-emission scanning electron microscope (FESEM) system was employed to analyze the resulting fractures in the coal specimens both before and after CO_2 fracturing. This was completed in the Henan International Joint Laboratory for Unconventional Energy Geology and Development. The SEM was manufactured by Carl Zeiss (Germany) with major specifications as listed in Table 3. Scanning observations used the high voltage (10.0kv) high resolution imaging model with backscattered electron (BSE) imaging utilized for improved resolution. A total of 23 samples were prepared for FESEM including five pristine (un-impacted) and 18 impacted samples.

Virgin coal samples were selected with bright vitrinite particles; particles from impacted samples were selected as $<$ 10 mm fragments from the thermoplastic sheath, or larger friable particles were broken by hand to meet the SEM requirement.

4. Results and discussion

4.1. Specimens after CO_2 gas impact

After treatment by CO_2 gas blasting, the specimens are damaged as shown in Fig. 4. It is expected that the intensity of damage progressively increases as the blasting pressure increases from 120 MPa to 185 MPa.

Table 3
The major parameters of the FESEM imaging.

Accelerating voltage (KV)	Magnification (10 K times)	Focus distance (mm)	resolving power (nm@15kv)	resolving power (nm@1kv)
0.02–30	12–40	0.1–50	0.8	1.6

The sample impacted at 120 MPa in Fig. 4A shows a half cracked cylindrical column as circled by the white line (Fig. 4A upper half), and half crushed fragment (Fig. 4A lower part) into small particles at centimeter to millimeter scale. The sample impacted by 185 MPa (Fig. 4C and 4D) shows considerably greater damage with centimeter to millimeter scale particles broken in form. At 150 MPa, the degree of damage (Fig. 4B) is intermediate between that at 120 to 185 MPa, and the cylindrical part was cracked with loosened fragments compared to those of Fig. 4A but still connected together.

4.2. Micro-scale coal damage evaluation from FESEM observation

4.2.1. Fractures in virgin coal samples

The morphology and micro-structures of the virgin coal without CO_2 blasting treatment are shown in Fig. 5. The structures are observed and classified as with **even and smooth** surface planes, cleats, pores and their combination. For the FESEM, all the impacted coal samples have been observed through a random manner. For the FESEM images, we focused on the qualitative fracture morphological analysis in this study with an intension of clarifying the effect of impact load on the fracture networks. Only representative data have been presented in this section.

Coal particle surface mostly shows simple **even and smooth plane** from millimeter scale to micrometer scale in this research (left areas of Fig. 5A and 5B). It is also found some arc lineation cross with radial lineation (in Fig. 5A right field) close to the left smooth plane, which may occur during a brittle broken. When we took high magnification, the arc lineation image shows ladder pattern structures, which is a combination of several even smooth plane steps (Fig. 5B).

Cleat formed with two cross straight fractures often appear shown in Fig. 5C, in which one fracture (F1) is open, and the second (F2) is filled with clay minerals. Different pores are frequently observed. Some single pores scatter in an even plane or as a group combined with many different size and shapes (Fig. 5D). Most of these pores are open without clay fillings.

Fig. 4. Damaged coal specimens after CO_2 gas impact at different pressures.

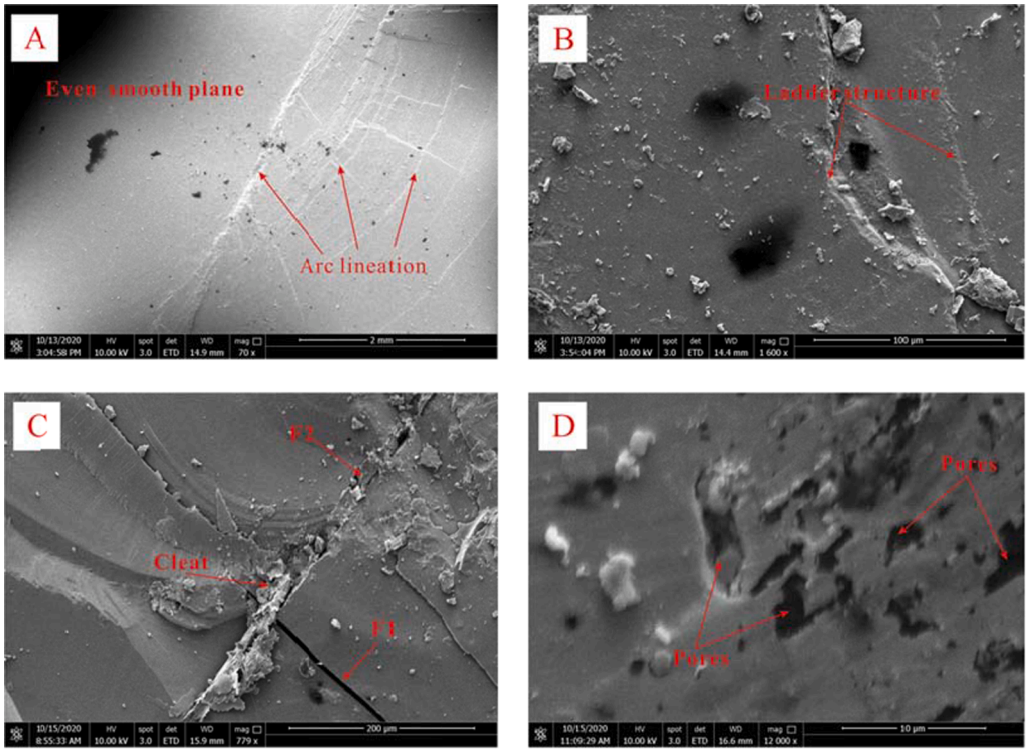

Fig. 5. SEM photos of microfractures in virgin coal (without CO_2 blasting). A: Even and smooth plane (left) with arc lineation (right); B: Even and smooth plane (left) with ladder pattern (right) formed from brittle crack. C: X pattern fractures or named cleats formed with two straight fractures: F1 is open and straight and F2 is straight but filled with clay type minerals. D: Pore group pattern showing many open pores gathering together with different size and shape.

4.2.2. Micro-fractures in CO_2 dynamically impacted coal

The micro-fracture system in the coal specimens after high pressure CO_2 impacting is much more complex, or multitudinous in the micrometer scale level. The most important new findings of this research are following 5 aspects.

(1) **Induced tri-radial-wing (TRW) fracture pattern.** This is the most important and popular fractures pattern in the blasting treated coal specimens. This pattern contains two key points: firstly, the tri-fracture pattern means most fractures newly developed by high pressure CO_2 gas impacting appear to be three single fracture shown as Fig. 6A, B, E, F, G and H. The three single fracture always initiate from one point, namely center point that circled by yellow lines in all images of Fig. 6. The length and open width of three fractures are different, one or two are greater than others. Secondly, the radial extending pattern means the three

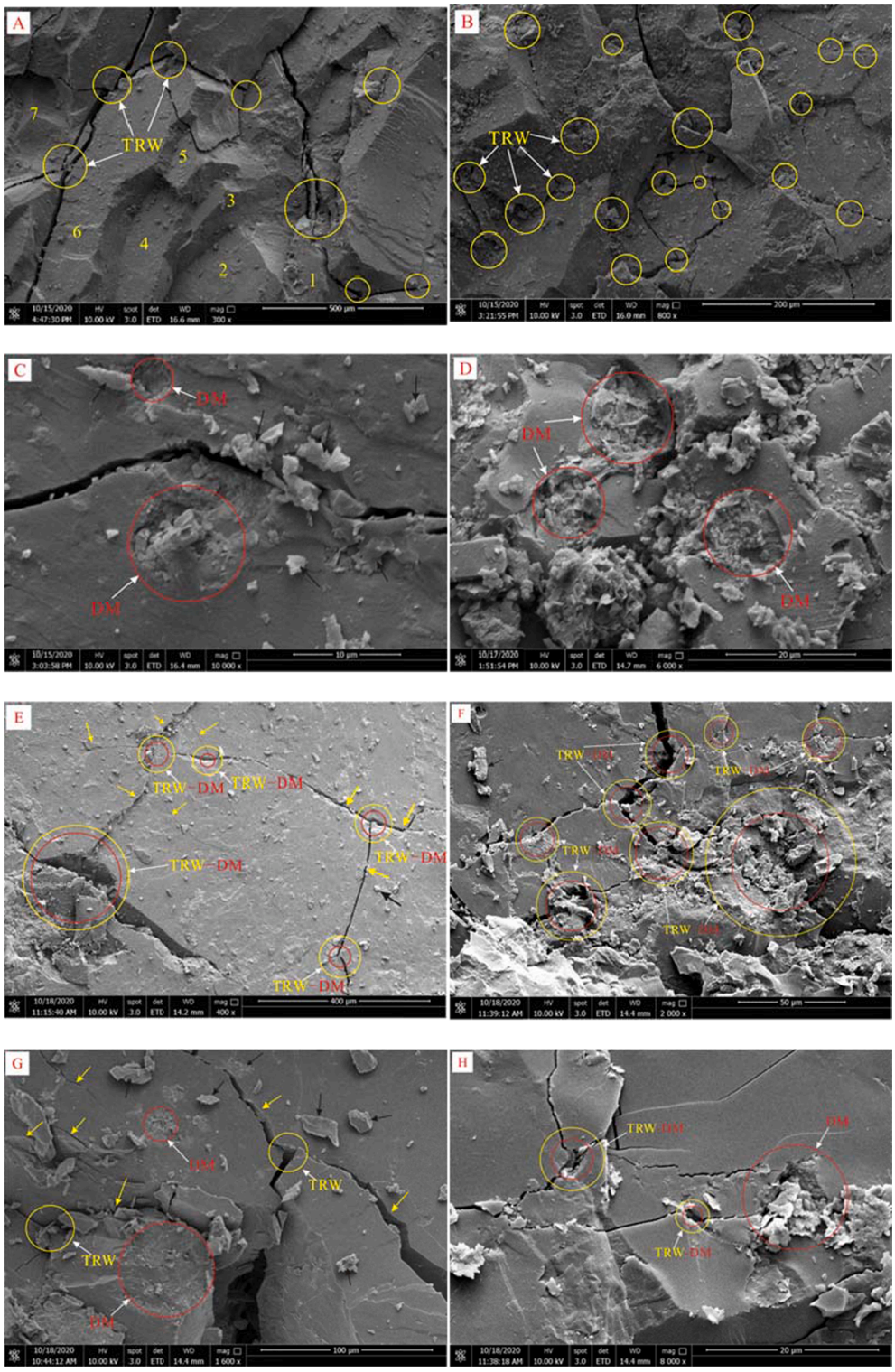

Fig. 6. SEM photos of microfractures in CO_2 dynamically-impacted coal. Impact pressures of: A-D: 120 MPa, E-H: 150 MPa.

single fracture mostly extend radially from the center point to three different directions. Even four fractures pattern (FRW) initiates from one center point and radial extending (Fig. 6A, B, E, F, G, H) was also found, but this is much less than the tri- fracture pattern. In the area of highly damaged, several tri-fracture pattern grouped together to be a fracture network (Fig. 6B, E, F, G), where high permeability can happen.

(2) **Damage mark (DM) at the center point of the tri- radial fracture pattern**. There always exists a distinct mark at the center point of the tri- radial fracture pattern circled with red line (Fig. 6C, D, E, F). All the three fractures exactly initiated from the mark center. The marks appear to be shallow pits showing damaged more serious with broken coal partial spared around the damage marks indicated with black arrow head (Fig. 6C, E, G). The damage mark size varies small and bigger, which is corresponding with the fracture size. Fig. 6C, D, F, G, H show that in high resolution view, damage marks always related with clear fracture system with long and open property. The density of the damage mark distributed varies largely from tens of micrometers (Fig. 6D, F, H) to hundreds of micrometers (Fig. 6A, E). On the other hands, not all the damage marks produce tri- radial fractures, but the most tri- radial fractures started from the mark point (Fig. 6E and F). The damage marks without fractures may imply that the fractures are too small to see at this condition, or the damage is not as enough to break the coal (Fig. 6G).

(3) **CO_2 gas is high pressure jet beam when impacting on coal**. From the observation of the FESEM view, the damage mark including its geometry property and tri- fractures initiation which reveals significant information of the CO_2 gas physic property when the gas impacting on coal. It is our understanding that the CO_2 gas is a high pressure and high velocity jet beam when the gas impacting on the coal or objective material. The damage marks are induced by CO_2 gas jet beam impaction. The distribution density of the gas jet beams may relate with the distance between the specimen and the CO_2 gas blowout nozzle. The distance is shorter, the jet beam is denser, and coal damage more serious. The damage mark size may relate with the gas jet beam thick, the thicker the jet beam, the bigger the damage mark is. We understand that the damage marks are the significant evidence that was produced by the high pressure CO_2 gas jet flow. Therefore, the mechanism of damage includes gas jet beam impacting on coal, then coal break from the impacting point, and finally tri-fractures initiate from the impact point.

(4) **Broken coal matrix particles.** In this study, the most important fracture pattern in virgin coal - cleats have not been observed in the treated coal, which indicates that cleat pattern of coal was fully destroyed by the CO_2 gas jet beam, and the coal we can see at the FESEM is matrix particle, and all the damage marks and the tri- radial fractures pattern occurred in the matrix particles. From the FESEM view, the coal particles are identified as vitrinite or semi-vitrinite particles. This is a very important finds, which means that coal permeability can be highly increased by CO_2 gas jet beam since the matrix is fractured as network state.

Except the above 4 findings, additional important observations are described as following two points. Firstly, the fractures CO_2 gas induced mostly are open and zigzag. As shown in Fig. 6, the newly formed fractures are open without any filling. The opening can be wide varying from several millimeter separating the sample in the eye observation level, but most fracture's opening is narrow in micrometer scale shown in Fig. 6. It is believed that these open fractures newly developed formed by tensile action, and the opening will highly increase permeability of the coal. Most fractures appear to be zigzag (Fig. 6F, G, H) or curve shape (Fig. 6E) in plane view, and straight fractures only appear in a short way here. It is deduced that the open zigzag fractures formed from extensile stress condition, may trace some hidden zigzag damage in the coal which was stimulated as high gas pressure impacting on the coal.

In Fig. 6, simples A to D are impacted by 120 MPa of CO2 gas, and E to G are impacted by 150 MPa. It is our understanding that the coal deformation mechanism in Fig. 6 belongs to impact-brittle-extend type, since the damage marks, the spare particles, and open zigzag tri-radial-wing fractures show brittle properties.

(5) **Flake (FL) and mortar (MO) texture.** The coal impacted by high CO_2 pressure of 185 MPa reveals a very different structure properties and deformation mechanism. The photos A, B and C in Fig. 7 shows flakes and mortars in different scale. The flake texture of coal here indicates very thin layer in nano meter scale in Fig. 7B and C, and the diameters vary largely in micrometer scale (Fig. 7C). The mortar size changes a lot from several micrometer (Fig. 7C MO3) to hundred micrometers (Fig. 7A MO2). In high magnification field, flakes appear evenly distributed circled with two white lines (Fig. 7C). In this study, it seems that the two structures of flake and mortar are appear together, flacks distributed in a complex fracture system that surrounding the mortars (Fig. 7A, B and C).

Fig. 7D shows another surface structure of coal fragment damaged by 185 MPa CO2 gas. This kind of plume structure can be found in most view of the coal particles. Yellow arow head indicates the shearing direction, and the white circle shows even smooth plane (Fig. 7D). This kind of structures have been found in fault or joint plane of hard sand rock or the igneous rock with fine mineral and even texture. It is an evidence revealing brittle and quick shearing broken action.

In the view of coal fragments impacted by 185 MPa CO_2 gas, we did not find tri-radial wing fracture and the damage marks. Furthermore, the flake structure was only found in the 185 MPa impacted coal, and has not found in the coal impacted by 120 to 150 MPa CO_2 gas. It is our understanding that the flake structure is the most heavily deformation result in coal in our study history either in this research or the naturally deformed coal by tectonic origin.

5. Discussion

It has been proven that the CARDOX can effectively induce long fracture in the field application and there are more than 50 mines are currently using this technology to increase the permeability of coal in China. One of the challenges of optimizing the field implementation is to understand the multi-scale fracture network initiation and propagation, which is the thrust of this study. Fractures/cleats in coal have been extensively investigated since it controls not only the coal permeability but the coal strength and integrity. In terms of coal permeability, it has be a major changes for the tight and tectonically deformation coal to have a natural permeability for the gas drainage. For the technically deformed coal, the naturally occurring cleats and tectonic deformed fractures are the two major fracture system, and bedding planes is another gas migration pathway which is closely related to coal deposition process [30–34]. Since all these three existing fracture systems are characterized as weak planes under the dynamic loads which are all potentially partially or fully destroyed by CO_2 gas jet beam, so that we did not recognize their damaged clues in this study under FESEM level.

Technically, coal formation fracturing is one of the most important techniques that can economically increase the permeability of coal and thus promote the gas drainage efficiency and gas production. Many different laboratory experiments and field demonstrations have been completed for hydraulic fracturing coal formation treatments [35–38], but only hydraulic fracturing and CO_2 gas fracturing were commercially adopted by coal mining industry. The laboratory physic simulation of coal fracturing by water-based technology provides direct evidence indicating fracture geometry and mechanism. A most recent study reported that hydraulic stimulating on anthracite coal did not produce new fractures, but only dilate the existing fractures in aperture, lengthen

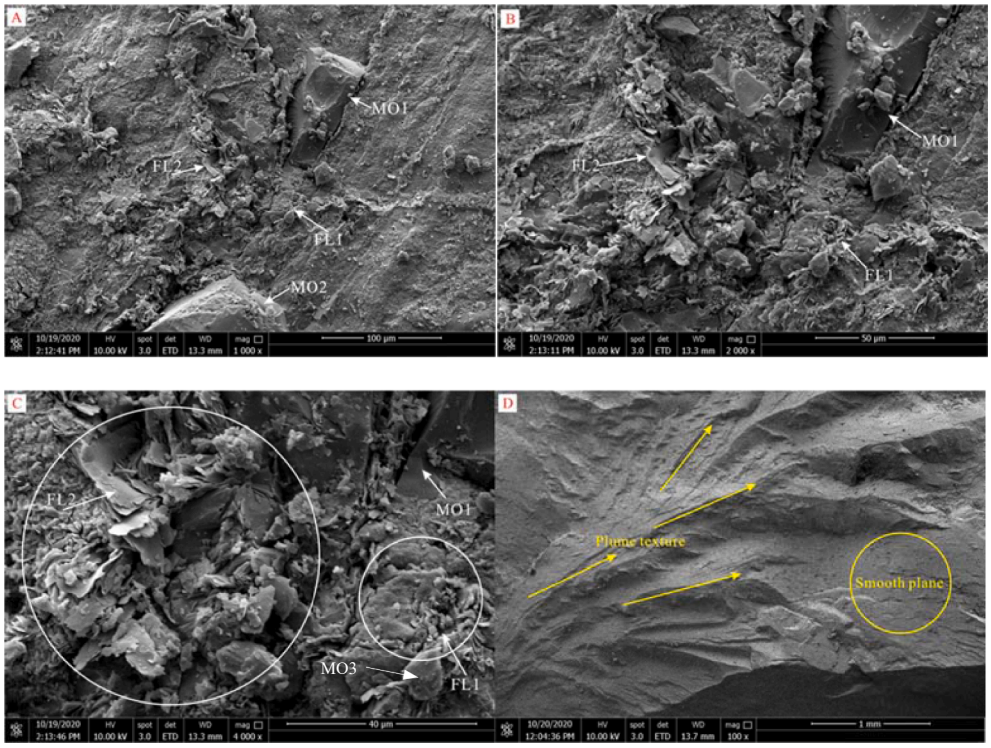

Fig. 7. SEM photos of microfractures in coal damaged by CO_2 gas blasting at 185 MPa.

and fracture porosity, and finally increase permeability [38]. These fracture size distributed in a range of 10 to 1000 μm. Obviously, CO_2 gas fracturing not only destroy the existing fractures like cleats/fractures, which will absolutely increase coal's permeability significantly, but also produce complex new fractures forming network within impacted coal matrices as observed in this study, which is the key difference with water-based hydraulic fracturing. Another laboratory stimulation experimental on bituminous coal by multi-cyclic hot/cold shock found millimeter scale fractures caused by shrink and expansion process when temperature changes and found that the large-scale fracture highly increased permeability [39,40], but the fracture mechanism is very different with CO_2 gas jet impacting. This cryogenic-fluid or super-hot fluid-based technologies are far away from field implementation due to its specific temperature requirements. Experiment of multiple cyclic liquid nitrogen freeze–thaw on coal reached a similar result as heating/cooling did, produced straight open crakes [41], which are also different with the fractures induced by CO_2 gas jet impacting in mechanism and fracture pattern. The fact is that these two kinds of technologies have only been demonstrated in the laboratory without direct adoption in the field scale pilot projects. Therefore, it is believed that CO_2 gas impacting is a very specific fracturing measure comparing with hydraulic, heating/cooling, and liquid nitrogen freeze and thaw.

This study showing that all the newly developed fractures observed under FESEM only within in matrix induced by high pressure CO_2 gas jetting. Coal matrices are observed as separated small cubic fragments by cleats and bedding fractures about millimeter to micrometer size. Matrix particles mostly composed with vitrinite and semi-vitrinite, which surface is clean, even and homogenous. When high CO_2 gas impact on matrix, tri-fracture system has been generated. Thus, two types of fractures produced by CO_2 gas fracturing: break or re-open the existing cleat or bedding system, and then damage the matrix particles forming tri-fracture networks.

Consequently, the matrix fracturing mechanism by high pressure (120 to 150 MPa) CO_2 gas blasting can be described as following (1) to (5) illustrated in Fig. 8.

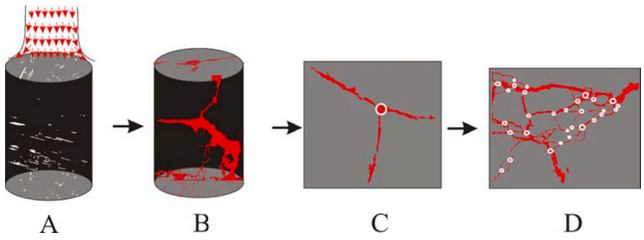

Fig. 8. A conceptual model of micro fracturing induced by CO_2 gas blasting with pressures of 120 MPa to 150 MPa.

(1) High pressure CO_2 gas ejects from the CARDOX tube nozzle forming massive amount of gas jet beams, which will be the impacting energy source due to the phase change;
(2) The gas jet beam impacting on coal specimen breaking the coal through cleat re-open, and then coal fully collapsed becoming small matrix particles in millimeter size.
(3) CO_2 gas beam impacting on the matrix particles forming DMs where are the locations with excessive dynamic failure, in which three fracture occurred and extending radially and the particle destroyed or collapsed in micrometer scale.
(4) When matrix particles broken, tri-fractures in multiple scale form a complex network where high stress in coal released and high permeability was built up (Fig. 7). Finally, gas drainage efficient will be highly improved.
(5) The high pressure of CARDOX (185 MPa) induce two different deformation in the anthracite coal. One is quick sheering broken forming the plume structure and second is observed to be a strong ductile sheering deformation forming the flake structures at nanoscale.

This study provides the direct visual fracture system through SEM in the scale of micrometer. It is observed that flake fractures in nanometer scale produced in the matrix also, and the CO_2 gas jet beam might

further open the nano scale porous, which will be an interesting research topic in the future.

6. Conclusions

High pressure CARDOX CO_2 gas blasting is a non-explosive blasting technology, and it can be safely employed in gassy coal mine environment for efficiently gas drainage. This technology is being used in coal industry for more than a century. The induced complex fracture system by CO_2 gas impacting are the primary mechanism for promoting the gas permeability and reduce the deviatoric stress for the virgin. The industry-scale field implementation over the past decade demonstrated that this technology has been and will be one of the most efficient measures for effective gas drainage in gas burst prone coal seams. We conducted field-scale (meters) CO_2 blasting experiments on anthracite and the microstructure of coal has been investigated by FESEM. The key findings are listed as the following.

1. Cleats can be observed only in the original coal specimens without CO_2 gas damage, and did not see in the samples damaged by CO_2 gas blasting. This phenomenon indicates that cleat system has been fully destroyed during the CO_2 gas impacting the coal. The SEM results demonstrate that the coal matrices were damaged by the impacted loads.
2. The two unique properties of micro-fractures induced by CO_2 impacting in coal matrix particle are tri-radial fracture pattern and the damage mark, which are very different with all other fractures induced by water-based fracturing techniques. The tri-radial fracture and damage mark are the essential elements for forming the interconnected fracture network and fluid pathways for the gas drainage.
3. Based on the geometry relationship of damage mark and the tri-fractures, it is evident that the CO_2 gas beam impacting can induce a tensile breaking regime on coal matrix followed by a radial micro-fracture propagation.
4. The highest CO_2 CARDOX pressure at 185 MPa can induce two different deformations: One is plume structure and second is the flack structures with nanometer scale layers, which may reveal a very strong ductile sheering deformation mechanism.

CRediT authorship contribution statement

Yunxing Cao: Conceptualization, Project administration, Funding acquisition, Supervision, Methodology, Writing – original draft. **Junsheng Zhang:** Visualization. **Xinsheng Zhang:** Visualization. **Shimin Liu:** Conceptualization, Methodology, Writing – review & editing. **Derek Elsworth:** Conceptualization, Methodology, Writing – review & editing.

Declaration of Competing Interest

The authors declare that they have no known competing financial interests or personal relationships that could have appeared to influence the work reported in this paper.

Acknowledgement

This research was financially supported by The Major National Science and Technology Projects in the 13th Five-year Plan (No. 2016ZX05067006-002; No. 2017ZX050674002).

References

[1] Feng Y, Li H, Du L, Li Y. 70 years' experience, effect, situation analysis and prospect of coal mine safety. China Coal 2014; 46(05): 47-56[In Chinese].
[2] Li RQ, Shi SL, Nian QF, Jiang M. Research on Coalmine Gas Accident Rules in China in Recent Decade. China Safety Science Journal 2011; 21(9): 143-51[In Chinese].
[3] Sun Q. Research on status quo and prevention countermeasures of coal mine gas disaster in China. China Coal 2014; 40(3): 116-9[In Chinese].
[4] Huang S. Perspectives and challenges of CBM/CMM industry in China. 13th International Symposium on CBM/CMM and Shale Gas in China, Beijing. 2013[In Chinese].
[5] Xie HP, Ju Y, Gao M, Gao F, Liu J, Ren H, et al. Theories and technologies for in-situ fluidized mining of deep underground coal. Journal of China Coal Society 2018; 43(05): 1210-9[In Chinese].
[6] Xie HP, Zhou HW, Xue DJ, Wang HW, Zhang R, Gao F. Research and consideration on deep coal mining and critical mining depth. Journal of China Coal Society 2012; 37(37): 535-42(8) [In Chinese].
[7] Safety State Administration Of Coal. AQ 1025–2006 2006 Specification for identification of classification of gaseous mines; 2006.
[8] Safety State Administration Of Coal. Guidance to Gas Drainage in Coal Mines.; 2011.
[9] Safety State Administration Of Coal. Safety Regulations in Coal Mines; 2014.
[10] Safety State Administration Of Coal. Provisions on Prevention and Control of Coal and Gas Outbursts; 2019.
[11] Safety State Administration Of Coal. Rules for the Prevention and Control of Coal and Gas Outburst; 2019.
[12] United Nations. Best practices guidance for effective methane drainage and use in coalmine. New York and Geneva, 2010, ECE Energy Series No. 31.
[13] Xu C, Cai F, Di C, Jia F. Experimental Study on Hydraulic Fracturing Permeability Improvement Technology in High Gas and Low Permeability Coal Seam. Coal Technol 2014; 33(05): 28-30[In Chinese].
[14] Lei L. Research on Application of Hydraulic Fracturing Test in Coal and Gas Outburst Coal. Coal Technol 2019; 38(03): 106-108[In Chinese].
[15] Chen XE, Cui XY, Dong-Ping TU, Zhang LJ. Application of Hydraulic Slot Cutting Technology to Improve Gas Drainage Effect. Coal Eng 2011;08:34–6.
[16] Fan YC, Wang ZF. Effect Analysis of Strengthening Permeability in Soft and Low Permeability Outburst Coal Seam by Hydraulic Flushing. Saf Coal Mines 2012; 43 (06): 137-40[In Chinese].
[17] Hu G, Wang X, Wang W. Study on technology of increasing permeability of low gas permeability coal seam by long-drilling explosion. J Heilongjiang Instit Sci Technol 2013; 23(02): 159-62[In Chinese].
[18] Liu MJ, Zhao WW, Liu YW, Wei JP. Research and Application of Hydraulic Flushing Borehole to Quickly Eliminate Outburst. Coal Sci Technol 2010; 38(03): 58-61[In Chinese].
[19] Liu YW, Ren PL, Xia SB, Sun YG. Analysis of pressure-relief and permeability improvement effect of hydraulic flushing. J Henan Polytechn Univers (Natl Sci) 2009; 28(06): 695-9[In Chinese].
[20] Song WY, Wang Z, Tang J. Principle of Gas Extraction by Increasing Permeability of Coal Seam with Hydraulic Cutting and Its Application. China Saf Sci J 2011; 21 (04):78-82[In Chinese].
[21] Li J, Lin B, Li G, Ye Q, Xu S. The theory and application of loose blasting for increasing permeability and distress in long boreholes. Coal Mine Safety 2010;52: 52-4[In Chinese].
[22] Li H, Lin B, Yang W, Gao Y, Liu T. Effects of an underlying drainage gallery on coal bed methane capture effectiveness and the mechanical behavior of a gate road. J Nat Gas Sci Eng 2015;27(part_P2):616–31.
[23] Szlązak N, Obracaj D, Swolkień J. Methane drainage from roof strata using an overlying drainage gallery. Int J Coal Geol 2014;136:99–115.
[24] Karacan CÖ. Integration of vertical and in seam horizontal well production analysis with stochastic geostatistical algorithms to estimate pre-mining methane drainage efficiency from coal seam: blue Creek seam, Alabama. Int J Coal Geol 2013;114 (Complete):96–113.
[25] Karacan CÖ, Diamond WP, Schatzel SJ. Numerical analysis of the influence of in-seam horizontal methane drainage boreholes on longwall face emission rates. Int J Coal Geol 2007;72(1):15–32.
[26] Cao Y, Tian L, Fan Y, Liu J, Zhang S. Study on cracking ring form of carbon dioxide gas phase fracturing in low permeability coal seam. Coal Sci Technol 2018; 46(06): 46-51[In Chinese].
[27] Cao Y, Zhang J, Tian L, Zhai H, Fu G, Tang J. Research and application of CO2 gas fracturing for gas control in low permeability coal seams. J China Coal Soc 2017; 42(10): 2631-41[In Chinese].
[28] Cao Y, Zhang J, Zhai H, Fu G, Tian L, Liu S. CO2 gas fracturing: A novel reservoir stimulation technology in low permeability gassy coal seams. Fuel 2017;203: 197–207.
[29] Iovr H. The blasting action of the CARDOX shell. Trans Inst Min Eng 1958;118: 1–19.
[30] Laubach SE, Marrett RA, Olson JE, Scott AR. Characteristics and origins of coal cleat: A review. Int J Coal Geol 1998;35(1–4):175–207.
[31] Peyman M, Ryan TA, Alireza G, Hu Y, Yu J, Fatemeh K, et al. Cleat-scale characterization of Coal: An overview. J Nat Gas Sci Eng 2017;39:143–60.
[32] Roslin A, Pokrajac D, Zhou Y. Cleat structure analysis and permeability simulation of coal samples based on micro-computed tomography (micro-CT) and scan electron microscopy (SEM) technology. Fuel 2019;254(OCT.15). 115579.1-.7.
[33] Zhao Y, Zhao G, Jiang Y, Elsworth D, Huang Y. Effects of bedding on the dynamic indirect tensile strength of coal: Laboratory experiments and numerical simulation. Int J Coal Geol 2014;132:81–93.
[34] Vassilev SV, Tascón JMD. Methods for Characterization of Inorganic and Mineral Matter in Coal: A Critical Overview. Energy Fuels 2003;17(2):271–81.
[35] Ni G, Dong K, Li S, Sun Q. Gas desorption characteristics effected by the pulsating hydraulic fracturing in coal. Fuel 2019;236:190–200.

[36] Tian L, Cao Y, Chai X, Liu T, Feng P, Feng H, et al. Best practices for the determination of low-pressure/permeability coalbed methane reservoirs, Yuwu Coal Mine, Luan mining area. China. Fuel 2015;160(nov.15). 100–7.
[37] Ge Z, Deng K, Zhou Z, Yang M, Chai C. Fracture characteristics of coal jointly impacted by multiple jets. Eng Fract Mech 2020;235:107171.
[38] Mou P, Pan J, Wang K, Wei J, Yang Y, Wang X. Influences of hydraulic fracturing on microfractures of high-rank coal under different in-situ stress conditions. Fuel 2021;287:119566.
[39] Zhang L, Lu S, Zhang C, Chen S. Effect of cyclic hot/cold shock treatment on the permeability characteristics of bituminous coal under different temperature gradients. J Nat Gas Sci Eng 2020;75:103121.
[40] Liu S, Wang D, Yin G, Li M, Li X. Experimental study on the microstructure evolution laws in coal seam affected by temperature impact. Rock Mech Rock Eng 2020;53(3):1359–74.
[41] Su S, Gao F, Cai C, Du M, Wang Z. Experimental study on coal permeability and cracking characteristics under LN2 freeze-thaw cycles. J Nat Gas Sci Eng 2020;83:103526.